

This article was downloaded by: [Renmin University of China]

On: 13 October 2013, At: 10:33

Publisher: Taylor & Francis

Informa Ltd Registered in England and Wales Registered Number: 1072954 Registered office: Mortimer House, 37-41 Mortimer Street, London W1T 3JH, UK



Journal of Coordination Chemistry

Publication details, including instructions for authors and subscription information:

<http://www.tandfonline.com/loi/gcoo20>

Hydrothermal synthesis and structural characterization of two new polytungstate-based hybrids

Zhan-Gang Han^a, Shan Li^a, Jing-Jing Wu^a & Xue-Liang Zhai^a

^a College of Chemistry and Material Science, Hebei Normal University, Shijiazhuang, Hebei 050016, China

Published online: 26 Apr 2011.

To cite this article: Zhan-Gang Han, Shan Li, Jing-Jing Wu & Xue-Liang Zhai (2011) Hydrothermal synthesis and structural characterization of two new polytungstate-based hybrids, Journal of Coordination Chemistry, 64:9, 1525-1532, DOI: [10.1080/00958972.2011.574696](https://doi.org/10.1080/00958972.2011.574696)

To link to this article: <http://dx.doi.org/10.1080/00958972.2011.574696>

PLEASE SCROLL DOWN FOR ARTICLE

Taylor & Francis makes every effort to ensure the accuracy of all the information (the "Content") contained in the publications on our platform. However, Taylor & Francis, our agents, and our licensors make no representations or warranties whatsoever as to the accuracy, completeness, or suitability for any purpose of the Content. Any opinions and views expressed in this publication are the opinions and views of the authors, and are not the views of or endorsed by Taylor & Francis. The accuracy of the Content should not be relied upon and should be independently verified with primary sources of information. Taylor and Francis shall not be liable for any losses, actions, claims, proceedings, demands, costs, expenses, damages, and other liabilities whatsoever or howsoever caused arising directly or indirectly in connection with, in relation to or arising out of the use of the Content.

This article may be used for research, teaching, and private study purposes. Any substantial or systematic reproduction, redistribution, reselling, loan, sub-licensing, systematic supply, or distribution in any form to anyone is expressly forbidden. Terms & Conditions of access and use can be found at <http://www.tandfonline.com/page/terms-and-conditions>

Hydrothermal synthesis and structural characterization of two new polytungstate-based hybrids

ZHAN-GANG HAN*, SHAN LI, JING-JING WU and XUE-LIANG ZHAI*

College of Chemistry and Material Science, Hebei Normal University,
Shijiazhuang, Hebei 050016, China

(Received 7 November 2010; in final form 8 March 2011)

Two new polytungstate-based compounds, $[\text{Co}(\text{mbpy})_3][\text{W}_6\text{O}_{19}]$ (**1**) and $[\text{Ni}(\text{mbpy})_2][\text{VW}_{12}\text{O}_{40}]$ (**2**) (mbpy = 4,4'-dimethyl-2,2'-bipyridyl), have been hydrothermally synthesized and characterized by IR spectroscopy, TG analysis, and single-crystal X-ray diffraction. Single crystal X-ray structural analyses demonstrate that the compounds consist of $[\text{M}(\text{mbpy})_3]^{2+}$ ($\text{M} = \text{Co}^{\text{II}}$ or Ni^{II}) as cations anchored to W-containing polyoxoanions through non-covalent intermolecular interactions. The inorganic polyanions exhibit different cluster structures: Lindqvist-type $[\text{W}_6\text{O}_{19}]^{2-}$ isopolyoxoanion in **1**; V-centered Keggin-type $[\text{VW}_{12}\text{O}_{40}]^{4-}$ heteropolyoxoanion in **2**.

Keywords: Polyoxometalate; Hydrothermal reaction; Lindqvist; Supramolecular interaction; Bipyridine

1. Introduction

Inorganic–organic hybrids attract interest due to the possibility of combining the different characteristics of the components to get unusual structures, properties, or applications [1, 2]. Polyoxometalates (POMs) with large size, various shapes, and rich electronic and magnetic properties are one of the most widely used inorganic components [3–7]. A popular synthetic strategy is to employ nucleophilic POMs as inorganic ligands to transition metal complexes (TMCs) for constructing hybrid frameworks [8]. Hybrids ranging from POMs modified by TMCs to frameworks based on POM building blocks covalently and/or non-covalently bridged by TMC moieties have been reported [9–12]. Compared with assemblies based on vanadium and molybdenum polyanions that have been extensively reported, tungsten-containing polyoxoanions are relatively limited [13–16].

Our research has focused on synthesis of POM-based assemblies through weak interactions which occur between surface oxygens of POMs and organic molecules [17]. Oxygens located on the surface endow POMs with opportunities to hydrogen bond with organic moieties. Therefore, polyanions may direct the assembly of the organic moiety through directional interactions involving N–H...O and C–H...O, etc.

*Corresponding author. Email: hanzgl16@yahoo.com.cn; xlzhai253@mail.hebtu.edu.cn

Bipyridines (bpy) have been widely used in POM chemistry. Using $-\text{CH}_3$ to decorate bpy would be beneficial to $\text{C}-\text{H}\cdots\text{O}$ interaction in assembling polyanions. Here 4,4'-dimethyl-2,2'-bipyridyl (mbpy) is used to construct POM-based supramolecular networks. This article reports the synthesis and crystal structures of two polytungstate-based hybrids, $[\text{Co}(\text{mbpy})_3][\text{W}_6\text{O}_{19}]$ (**1**) and $[\text{Ni}(\text{mbpy})_3]_2[\text{VW}_{12}\text{O}_{40}]$ (**2**). Two compounds consist of different anionic clusters, Lindqvist $[\text{W}_6\text{O}_{19}]^{2-}$ isopolyoxoanion in **1** and V-centered Keggin-type $[\text{VW}_{12}\text{O}_{40}]^{4-}$ heteropolyoxoanion in **2**. They exhibit different supramolecular frameworks based on non-covalent interactions. There are extensive and effective intermolecular hydrogen bonding interactions among inorganic and organic moieties in both compounds.

2. Experimental

2.1. Materials and physical measurements

All chemicals were of reagent grade and used without purification. Elemental analyses were carried out on a Perkin Elmer 2400 CHN elemental analyzer. IR spectra were recorded from 400 to 4000 cm^{-1} on an Alpha Centaur FTIR spectrophotometer using a KBr pellet. TG analysis was performed on a Perkin Elmer Pyris Diamond TG/DTA instrument in flowing N_2 with a heating rate of $10^\circ\text{C min}^{-1}$.

2.2. Syntheses of **1** and **2**

2.2.1. Synthesis of $[\text{Co}(\text{mbpy})_3][\text{W}_6\text{O}_{19}]$ (1**).** A mixture of $\text{Na}_2\text{WO}_4\cdot 2\text{H}_2\text{O}$ (330 mg, 1.0 mmol), mbpy (45 mg, 0.25 mmol), $\text{CoCl}_2\cdot 6\text{H}_2\text{O}$ (96 mg, 0.4 mmol) and H_2O (12 mL) was stirred at room temperature for 25 min. The final pH was adjusted to ~ 4 with 4 mol L^{-1} HCl, and then the mixture was sealed in an 18 mL Teflon-lined steel autoclave and heated at 180°C for 5 days. After cooling to room temperature, yellow block crystals were obtained in 28% yield (based on W). Anal. Calcd for **1** (%): C, 21.40; H, 1.78; and N, 4.16. Found: C, 21.41; H, 1.70; and N, 4.21. IR(cm^{-1}): 3447(s), 1653(m), 1448(s), 1136(s), 994(w), 955(w), 876(w), 800(w), 617(w), 554(s), and 447(w).

2.2.2. Synthesis of $[\text{Ni}(\text{mbpy})_3]_2[\text{VW}_{12}\text{O}_{40}]$ (2**).** A mixture of V_2O_5 (45 mg, 0.25 mmol), $\text{Na}_2\text{WO}_4\cdot 2\text{H}_2\text{O}$ (660 mg, 2.0 mmol), $\text{NiSO}_4\cdot 6\text{H}_2\text{O}$ (263 mg, 1.0 mmol), mbpy (45 mg, 0.25 mmol), and H_2O (12 mL) was stirred at room temperature for 25 min. The final pH was adjusted to ~ 5 with 4 mol L^{-1} HCl, and then the mixture was sealed in an 18 mL Teflon-lined steel autoclave and heated at 180°C for 5 days. After cooling to room temperature, black crystals were obtained in 22% yield (based on W). Anal. Calcd for **2** (%): C, 20.97; H, 1.75; and N, 4.08. Found: C, 20.86; H, 1.79; and N, 4.19. IR(cm^{-1}): 3446(s), 3126(s), 2361(s), 1617(m), 1399(s), 970(w), 896(m), 779(m), 669(m), 519(w), 448(w).

2.3. X-ray crystallography

Data on crystals of **1** and **2** were collected at 298 K with a Bruker Smart Apex CCD diffractometer with Mo-K α monochromated radiation ($\lambda = 0.71073 \text{ \AA}$). Cell constants and orientation matrices for data collection were obtained from the least-squares refinements of setting angles in the range $1.57^\circ \leq \theta \leq 25.01^\circ$ for **1** and $1.88^\circ \leq \theta \leq 25.01^\circ$ for **2**. The structures were solved by direct methods and refined by full-matrix least-squares on F^2 using the SHELXTL crystallographic software package [18]. Anisotropic thermal parameters were used to refine all non-hydrogen atoms. Positions of hydrogens attached to carbons were fixed at their ideal positions. Crystal data and structure refinement parameters of **1** and **2** are listed in table 1. CCDC reference numbers: 797423 for **1** and 797424 for **2**.

3. Results and discussion

3.1. Synthesis

Hydrothermal synthesis has developed as a popular method for preparation of inorganic–organic composite solid materials. Under hydrothermal conditions, new phases are often obtained with previously unseen compositions and topologies [19]. In a specific hydrothermal process, many factors influence the final crystal phases, such as

Table 1. Crystal data and structure refinement parameters for **1** and **2**.

Compound	1	2
Empirical formula	C ₃₆ H ₃₆ CoN ₆ O ₁₉ W ₆	C ₇₂ H ₇₂ N ₁₂ Ni ₂ O ₄₀ VW ₁₂
Formula weight	2018.74	4119.98
Temperature (K)	296(2)	298(2)
Crystal system	Orthorhombic	Monoclinic
Space group	<i>Pccn</i>	<i>C2/c</i>
Unit cell dimensions (\AA , $^\circ$)		
<i>a</i>	37.9782(13)	26.016(3)
<i>b</i>	10.9265(4)	13.2539(18)
<i>c</i>	21.6669(7)	27.337(3)
α	90	90
β	90	95.9430(10)
γ	90	90
Volume (\AA^3), <i>Z</i>	8991.1(5), 8	9375.3(19), 4
Calculated density (Mg m^{-3})	2.983	2.919
Absorption coefficient (mm^{-1})	15.729	15.229
<i>F</i> (000)	7336	7500
Crystal size (mm^3)	$0.26 \times 0.19 \times 0.18$	$0.28 \times 0.20 \times 0.12$
Limiting indices	$-42 \leq h \leq 45$; $-12 \leq k \leq 12$; $-23 \leq l \leq 25$	$-30 \leq h \leq 30$; $-15 \leq k \leq 11$; $-32 \leq l \leq 32$
Reflections collected	54,829	22,776
Independent reflections	7861 [<i>R</i> (int) = 0.0347]	8220 [<i>R</i> (int) = 0.1199]
Goodness-of-fit on F^2	0.917	1.069
Final <i>R</i> indices [$I > 2\sigma(I)$]	$R_1 = 0.0507$, $wR_2 = 0.1542$	$R_1 = 0.0818$, $wR_2 = 0.1803$
<i>R</i> indices (all data)	$R_1 = 0.0610$, $wR_2 = 0.1697$	$R_1 = 0.1677$, $wR_2 = 0.2603$

initial reactant, initial concentration, pH, reaction time, temperature, etc. In our case, parallel experiments reveal that the initial reactants and concentrations greatly influence the structures of products.

Compound **1** was separated from the hydrothermal reaction of $\text{Na}_2\text{WO}_4 \cdot 2\text{H}_2\text{O}$, mbpy, $\text{CoCl}_2 \cdot 6\text{H}_2\text{O}$ and H_2O at 180°C for 5 days. The structure of **1** is built on $[\text{W}_6\text{O}_{19}]^{2-}$ and $[\text{Co}(\text{mbpy})_3]^{2+}$. Using $\text{NiSO}_4 \cdot 6\text{H}_2\text{O}$ instead of $\text{CoCl}_2 \cdot 6\text{H}_2\text{O}$ and adding V_2O_5 and then adjusting the mole ratio resulted in Keggin-type anion in **2**. WO_4^{2-} tends to polymerize to form isopolytungstates of different size and shape under acid conditions and may also polymerize with phosphate, silicate, vanadate, etc. to form heteropolytungstates. Our experiments showed that the reactions must occur at $\text{pH} \approx 4$ or 5 aqueous solutions. In a lower pH range (less than 3.8) or in a higher pH range (larger than 5.2), the compounds were not isolated. So pH is a very important factor in syntheses of **1** and **2**.

Several examples had shown that some accessory ingredients, such as NH_4VO_3 [20] and Na_2VO_3 [21], were necessary for the formation of inorganic–organic hybrids based on $[\text{W}_6\text{O}_{19}]^{2-}$ polyanion and bpy. The isolation of **1** indicates that this kind of hybrid may also be prepared without the accessory ingredient. Introduction of V plays a crucial role in forming the Keggin-type structure in **2**.

3.2. Structural description

X-ray structural analysis reveals that the basic unit of **1** consists of one $[\text{W}_6\text{O}_{19}]^{2-}$ and one $[\text{Co}(\text{mbpy})_3]^{2+}$ (figure 1), which are connected by intermolecular C–H...O interactions into a 3D supramolecular structure. The Lindqvist polyoxoanion is formed by six $\{\text{WO}_6\}$ octahedra connected through edge-sharing oxygens and thus exhibits approximate O_h symmetry. In **1**, there are two different orientations for isopolyanions: O(20)- and O(21)-centered $[\text{W}_6\text{O}_{19}]^{2-}$ clusters. $[\text{W}_6\text{O}_{19}]^{2-}$ consists of three kinds of oxygens, terminal oxygen (O_a), double-bridging oxygen (O_b), and central oxygen (O_c). Therefore, W–O band lengths can be grouped into three sets: W– O_a

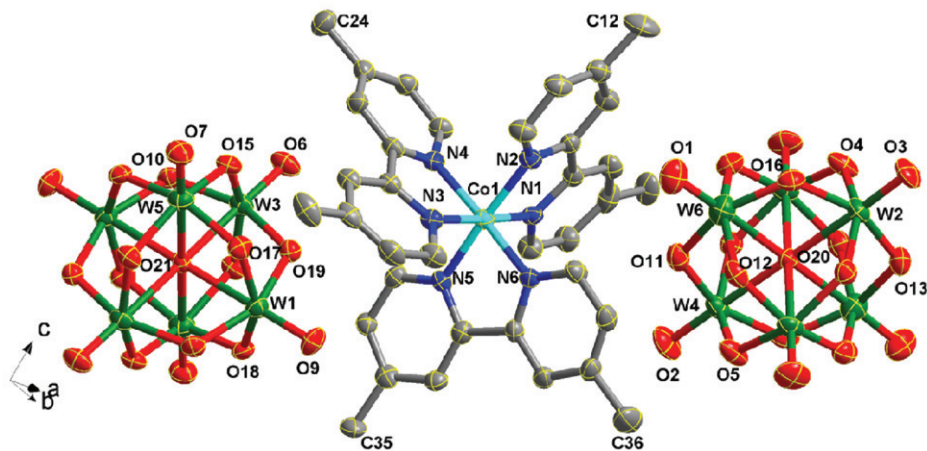


Figure 1. ORTEP view with 50% thermal ellipsoid probability showing the Lindqvist-type $[\text{W}_6\text{O}_{19}]^{2-}$ isopolyoxoanion and $[\text{Co}(\text{mbpy})_3]^{2+}$ cation in **1**.

1.666(14)~1.716(10) Å; W–O_b 1.877(9)~1.951(11) Å; and W–O_c 2.2876(8)~2.3135(5) Å. Comparing with those of classical Lindqvist isopolyanion salts, W–O bond distances in **1** have only slight changes. The Co(II) is octahedrally coordinated by six nitrogens from three mbpy ligands. The [Co(mbpy)₃]²⁺ coordination octahedron is slightly distorted, with Co–N bond lengths of 1.915(9)~1.944(11) Å.

Intermolecular hydrogen bonds occur among the anions and Co-mbpy cations. Some representative hydrogen bond distances for **1** are listed in table 2. As shown in figure 2, the two different orientations of [W₆O₁₉]²⁻ are surrounded with different environments formed by [Co(mbpy)₃]²⁺. The Co...Co distances are 10.979 × 10.933 and 9.783 × 10.927 Å, respectively. A 3D wave-shaped arrangement is constructed through supramolecular interactions among surface oxygens of [W₆O₁₉]²⁻ and [Co(mbpy)₃]²⁺ (figure 3). The isopolyanions are in grids formed by Co-ligand units, exhibiting a –A–B–C–D-type arrangement.

Single crystal analysis revealed that **2** is monoclinic space group C_{2/c} and consists of one V-centered Keggin-type polyoxoanion [VW₁₂O₄₀]⁴⁻ and two [Ni(mbpy)₃]²⁺. [VW₁₂O₄₀]⁴⁻ exhibits a V-center α-Keggin structure [22]. The anion may be viewed as a shell of {W₁₂O₃₆} encapsulating a {VO₄} responsible for the local T_d point symmetry of whole Keggin cluster. The central V atom is tetrahedrally coordinated with two crystallographically disordered orientations in a 1:1 ratio. The V–O distances range from 1.65(4) to 1.76(5) Å (mean value: 1.694 Å). The twelve {WO₆} octahedra are linked by sharing oxygens. All tungstens exhibit a VI oxidation state and have similar distorted octahedral environments with W–O_d bond lengths 1.58(3)~1.68(3) Å, W–O_{b/c} bond lengths 1.81(3)~1.94(3) Å and W–O_c bond lengths 2.26(4)~2.51(5) Å. In [Ni(mbpy)₃]²⁺, each Ni²⁺ is connected with three mbpy ligands in a distorted octahedral geometry. The Ni coordination octahedron has bond lengths of Ni–N = 2.07(3)~2.14(3) Å and angles of N–Ni–N = 78.5(10)~172.7(11)°. As shown in

Table 2. Some representative hydrogen bonding distances in **1–2**.

D–H...A (Å)	D–H (Å)	H...A (Å)	D...A (Å)	∠D–H...A (°)
Compound 1				
C(9)–H(9A)...O(16 ⁱ)	0.93	2.23	3.089(19)	153
C(21)–H(21A)...O(15 ⁱⁱ)	0.93	2.58	3.442(16)	154
C(24)–H(24A)...O(7 ⁱⁱ)	0.96	2.50	3.45(2)	169
C(23)–H(23A)...O(3 ⁱⁱⁱ)	0.96	2.42	3.24(2)	144
C(31)–H(31A)...O(3 ^{iv})	0.93	2.31	3.219(19)	166
C(34)–H(34A)...O(1)	0.93	2.49	3.26(2)	140
Compound 2				
C(2)–H(2)...O(10 ⁱ)	0.93	2.46	3.35(4)	162
C(5)–H(5)...O(20)	0.93	2.55	3.38(4)	149
C(14)–H(14)...O(16 ⁱⁱ)	0.93	2.59	3.50(5)	167
C(20)–H(20)...O(16 ⁱⁱⁱ)	0.93	2.55	3.47(5)	174
C(28)–H(28)...O(21 ⁱⁱⁱ)	0.93	2.49	3.26(4)	140
C(30)–H(30B)...O(21 ⁱⁱⁱ)	0.96	2.45	3.35(4)	155
C(26)–H(26)...O(19 ^{iv})	0.93	2.54	3.47(4)	177
C(32)–H(32)...O(19 ^{iv})	0.93	2.57	3.38(5)	146

Symmetry code for Compound **1**: i = 1/2 – x, 3/2 – y, z; ii = –x, 1/2 + y, 3/2 – z; iii = 1/2 – x, –1 + y, 1/2 + z; iv = 1/2 – x, y, –1/2 + z.

Symmetry code for Compound **2**: i = –x, y, 1/2 – z; ii = x, 1 + y, z; iii = 1/2 – x, 1/2 + y, 1/2 – z; iv = 1/2 – x, 1/2 – y, –z.

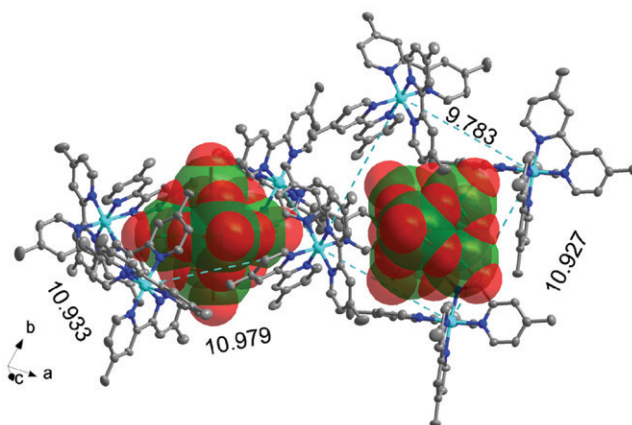


Figure 2. Four $[\text{Co}(\text{mbpy})_3]^{2+}$ surround one $[\text{W}_6\text{O}_{19}]^{2-}$ anion, showing the intermolecular hydrogen bonding interactions in **1**.

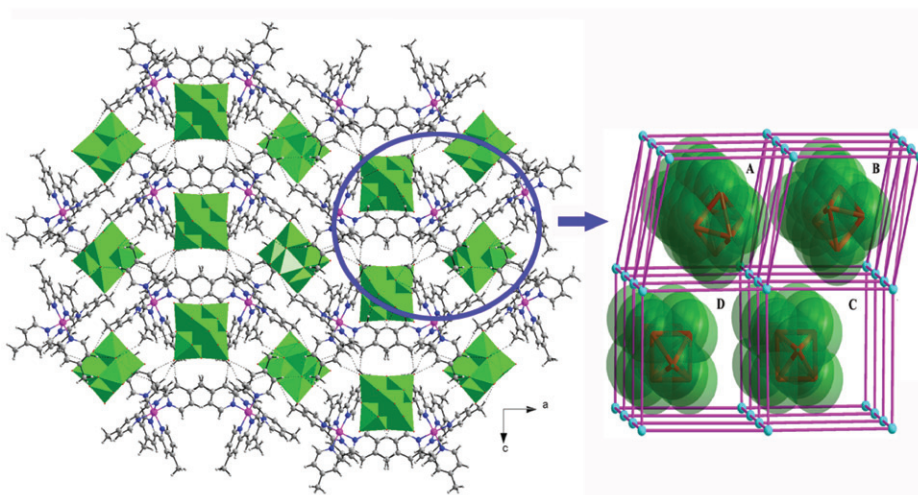


Figure 3. View showing the 3D supramolecular structure of **1**.

figure 4, four $[\text{Ni}(\text{mbpy})_3]^{2+}$ around one $[\text{VW}_{12}\text{O}_{40}]^{4-}$ have $\text{Ni}\cdots\text{Ni}$ distances of 12.981×14.599 Å. The longer $\text{Ni}\cdots\text{Ni}$ distances than $\text{Co}\cdots\text{Co}$ in **1** arise from different sizes of anions. The $[\text{VW}_{12}\text{O}_{40}]^{4-}$ and $[\text{Ni}(\text{mbpy})_3]^{2+}$ are linked into a 3-D supramolecular network through intermolecular hydrogen bonding interactions ($\text{C-H}\cdots\text{O} = 3.26(4) \sim 3.50(5)$ Å) (table 2).

3.3. IR spectroscopy

IR spectra for **1** and **2** display bands attributable to $\nu(\text{W}-\text{O}_t)$, $\nu(\text{W}-\text{O}_b-\text{W})$ and $\nu(\text{W}-\text{O}_c)$ at 955, 876, and 447 cm^{-1} for **1**; 970, 896, 779, and 448 cm^{-1} for **2**. A number of absorptions at 1399–1623 cm^{-1} are attributed to mbpy. A series of broad peaks at 3000–3500 cm^{-1} may be assigned to C–H stretch.

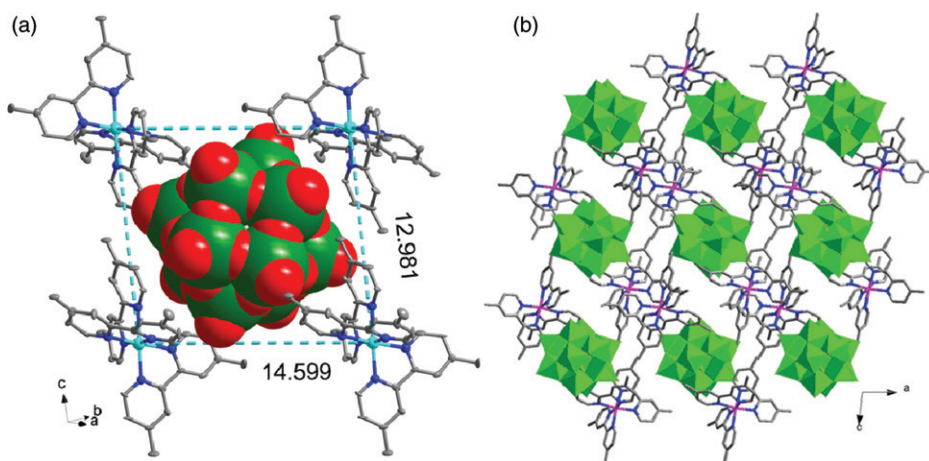


Figure 4. (a) View of four $[\text{Ni}(\text{mbpy})_3]^{2+}$ surrounding one $[\text{VW}_{12}\text{O}_{40}]^{4-}$; (b) view showing the 3D supramolecular structure of **2**.

3.4. Thermogravimetric analysis (TGA)

Thermal stability of **1** and **2** were investigated on crystalline samples under N_2 with a heating rate of $10^\circ\text{C min}^{-1}$ from room temperature to 800°C (Supplementary material). The TGA curve of **1** indicates two steps that are almost continuous. Total weight loss of 29.96% (Calcd 27.34%) between 330°C and 610°C is attributed to decomposition of mbpy. The TGA curve of **2** indicates a two-step continuous weight loss of 18.67% (Calcd 19.47%) between 175°C and 730°C , attributed to decomposition of mbpy.

4. Conclusions

Two new polytungstate-based hybrids (**1** and **2**) containing $[\text{M}(\text{mbpy})_3]^{2+}$ have been synthesized under hydrothermal conditions. The compounds consist of different polyanions, $[\text{W}_6\text{O}_{19}]^{2-}$ in **1** and $[\text{VW}_{12}\text{O}_{40}]^{4-}$ in **2**. The results indicated that using $-\text{CH}_3$ on bpy is beneficial to construct the POM-based supramolecular assemblies. Research on tungsten-containing polyoxoanions will be continued to obtain hybrids combining the features of both POM and TMC.

Supplementary material

Figures S1–S4 show the IR and XRD curves for **1** and **2**; figure S5 shows the TGA curves of **1** and **2**. Crystallographic data have been deposited with the Cambridge Crystallographic Data Center with the CCDC reference numbers 797423 and 797424 for **1** and **2**, respectively. These data can be obtained free of charge from the Cambridge Crystallographic Data Centre *via* www.ccdc.cam.ac.uk/data_request/cif.

Acknowledgments

This work was financially supported by the Natural Science Foundation of China (no. 20701011), Doctoral Initial Foundation of Hebei Normal University (no. L2005B13), the Hebei Natural Science Foundation of China (no. B2011205035), and the Education Department Foundation of Hebei Province (no. Z2006436).

References

- [1] (a) H.N. Miras, G.J.T. Cooper, D.L. Long, H. Bögge, A. Müller, C. Streb, L. Cronin. *Science*, **327**, 72 (2010); (b) P.P. Mishra, J. Pigga, T.B. Liu. *J. Am. Chem. Soc.*, **130**, 1548 (2008); (c) Q.S. Yin, J.M. Tan, C. Besson, Y.V. Geletii, D.G. Musaev, A.E. Kuznetsov, Z. Luo, K.I. Hardcastle, C.L. Hill. *Science*, **328**, 342 (2010).
- [2] (a) R. Tsunashima, D.L. Long, H.N. Miras, D. Gabb, C.P. Pradeep, L. Cronin. *Angew. Chem., Int. Ed.*, **49**, 113 (2010); (b) G.G. Gao, P.S. Cheng, T.C.W. Mak. *J. Am. Chem. Soc.*, **131**, 18257 (2009).
- [3] (a) J.Q. Sha, J. Peng, H.S. Liu, J. Chen, A.X. Tian, P.P. Zhang. *Inorg. Chem.*, **46**, 11183 (2007); (b) X.L. Wang, C. Qin, E.B. Wang, Z.M. Su, Y.G. Li, L. Xu. *Angew. Chem., Int. Ed. Engl.*, **45**, 7411 (2006).
- [4] Y.Q. Lan, S.L. Li, X.L. Wang, K.Z. Shao, D.Y. Du, H.Y. Zang, Z.M. Su. *Inorg. Chem.*, **47**, 8179 (2008).
- [5] H.Y. An, E.B. Wang, D.R. Xiao, Y.G. Li, Z.M. Su, L. Xu. *Angew. Chem., Int. Ed. Engl.*, **45**, 904 (2006).
- [6] X.L. Wang, Y.F. Bi, B.K. Chen, H.Y. Lin, G.C. Liu. *Inorg. Chem.*, **47**, 2442 (2008).
- [7] Y.P. Ren, X.J. Kong, L.S. Long, R.B. Huang, L.S. Zheng. *Cryst. Growth Des.*, **6**, 572 (2006).
- [8] (a) J.W. Zhao, H.P. Jia, J. Zhang, S.T. Zheng, G.Y. Yang. *Chem. Eur. J.*, **13**, 10030 (2007); (b) S.T. Zheng, J. Zhang, G.Y. Yang. *Angew. Chem., Int. Ed. Engl.*, **47**, 3909 (2008).
- [9] (a) P.J. Hagrman, D. Hagrman, J. Zubietta. *Angew. Chem., Int. Ed.*, **38**, 2638 (1999); (b) F. Yao, F.X. Meng, Y.G. Chen, C.J. Zhang. *J. Coord. Chem.*, **63**, 196 (2010).
- [10] C.M. Liu, D.Q. Zhang, D.B. Zhu. *Cryst. Growth Des.*, **6**, 524 (2006).
- [11] Q.G. Zhai, X.Y. Wu, S.M. Chen, Z.G. Zhao, C.Z. Lu. *Inorg. Chem.*, **46**, 5046 (2007).
- [12] (a) Z.G. Han, Y.L. Zhao, J. Peng, H.Y. Ma, Q. Liu, E.B. Wang, N.H. Hu, H.Q. Jia. *Eur. J. Inorg. Chem.*, 264 (2005); (b) Z.G. Han, T. Chai, X.L. Zhai, J.Y. Wang, C.W. Hu. *Solid State Sci.*, **11**, 1998 (2009).
- [13] (a) Z.G. Han, J.J. Wu, T. Chai, X.L. Zhai. *J. Coord. Chem.*, **63**, 1690 (2010); (b) Y.Z. Zhou, H.P. Qiao. *Inorg. Chem. Commun.*, **10**, 1318 (2007).
- [14] B.E. Koene, N.J. Taylor, L.F. Nazar. *Angew. Chem., Int. Ed.*, **38**, 2888 (1999).
- [15] W.W. Li, Q. Wang, W.S. You, L.J. Qi, L.M. Dai, Y. Fang. *Inorg. Chem. Commun.*, **12**, 1185 (2009).
- [16] (a) S.Y. Zhang, L.J. Ci, H.R. Liu. *J. Phys. Chem. C*, **113**, 8624 (2009); (b) G. Ferey. *Chem. Mater.*, **13**, 3084 (2001).
- [17] (a) Z.G. Han, Y.G. Gao, X.L. Zhai, J. Peng, A.X. Tian, Y.L. Zhao, C.W. Hu. *Cryst. Growth Des.*, **9**, 1225 (2009); (b) Z.G. Han, Y.G. Gao, C.W. Hu. *Cryst. Growth Des.*, **8**, 1261 (2008); (c) Z.G. Han, Y.L. Zhao, J. Peng, A.X. Tian, Q. Liu, J.F. Ma, E.B. Wang, N.H. Hu. *Cryst. Eng. Comm.*, **7**, 380 (2005); (d) Z.G. Han, Y.L. Zhao, J. Peng, A.X. Tian, Y.H. Feng, Q. Liu. *J. Solid State Chem.*, **178**, 1386 (2005); (e) Z.G. Han, Y.L. Zhao, J. Peng, H.Y. Ma, Q. Liu, E.B. Wang, N.H. Hu. *J. Solid State Chem.*, **177**, 4325 (2004); (f) Z.G. Han, Y.L. Zhao, J. Peng, H.Y. Ma, Q. Liu, E.B. Wang. *J. Mol. Struct.*, **738**, 1 (2005).
- [18] (a) G.M. Sheldrick. *SHELXS-97, Program for Crystal Structure Solution*, University of Göttingen, Göttingen, Germany (1997); (b) G.M. Sheldrick. *SHELXL-97, Program for Crystal Structure Refinement*, University of Göttingen, Göttingen, Germany (1997).
- [19] (a) B.B. Yan, Y. Xu, X.H. Bu, N.K. Goh, L.S. Chia, G.D. Stucky. *J. Chem. Soc., Dalton Trans.*, 2009 (2001); (b) Y.K. Ku, X.B. Cui, J.N. Xu, Q. Gao, Y. Chen, J. Jin, S.Y. Shi, J.Q. Xu, T.G. Wang. *J. Coord. Chem.*, **63**, 394 (2010).
- [20] P.T. Ma, C.F. Yu, J.W. Zhao, Y.Q. Feng, J.P. Wang, J.Y. Niu. *J. Coord. Chem.*, **62**, 3117 (2009).
- [21] W.L. Chen, Y.H. Wang, Y.G. Li, E.B. Wang, Y.W. Li. *J. Coord. Chem.*, **62**, 1035 (2009).
- [22] (a) M.I. Khan, S. Cevik. *J. Chem. Soc., Dalton Trans.*, 1651 (1999); (b) M.X. Yang, S. Lin, L.J. Chen, X.F. Zhang, H.H. Xu. *Inorg. Chem. Commun.*, **12**, 566 (2009); (c) M.X. Yang, S. Lin, X.H. Chen, M.H. Luo, J.H. Liu. *J. Coord. Chem.*, **63**, 406 (2010).